Extraction of axial mass and strangeness values from the MiniBooNE neutral current elastic cross section measurement

Tomasz Golan, Krzysztof M. Graczyk, Cezary Juszczak, and Jan T. Sobczyk
Institute of Theoretical Physics, Wrocław University Plac Maxa Borna 9, 50-204 Wrocław, Poland
(Received 23 February 2013; revised manuscript received 12 July 2013; published 16 August 2013)

Results of the analysis of the MiniBooNE experiment data for the neutral current elastic neutrino scattering off the CH_2 target with the NuWro Monte Carlo generator are presented. The inclusion in the analysis of the two-body current contribution leads to the axial mass value $M_A = 1.10^{+0.13}_{-0.15}$ GeV, consistent with the older evaluations based on the neutrino-deuteron scattering data. The strange quark contribution to the nucleon spin is estimated with the value $g_A^s = -0.4^{+0.5}_{-0.3}$.

DOI: 10.1103/PhysRevC.88.024612 PACS number(s): 13.15.+g, 13.40.Gp, 24.10.Lx, 12.15.Mm

I. INTRODUCTION

There has been a lot of interest in neutrino interactions in the few-GeV energy region, coming from oscillation experiments and the demand to better constrain the systematic errors. For neutrino energies around 1 GeV the most abundant reaction is charged current quasielastic (CCQE) scattering, $\nu_\mu + n \to \mu^- + p$, and it is also the most important process in the investigation of the oscillation phenomenon, e.g., in the T2K Collaboration experiment [1].

Owing to the standard conserved vector current (CVC) and partially conserved axial current (PCAC) hypotheses, using the electron scattering data and assuming a dipole form of the axial form factor, the weak transition matrix element contains only one unknown parameter, the axial mass M_A. Recent neutrino CCQE cross section measurements, notably the high statistics muon double differential cross section results from the MiniBooNE (MB) experiment [2], suggest M_A values significantly larger than estimations from the older deuteron target neutrino measurements and from the pion electroproduction data [3]. It is becoming clear that in order to understand correctly the MB data, a two-body current contribution to the cross section must be considered [4–7]. In the experimental event identification this contribution can easily be confused with genuine CCQE events. The older and recent CCQE M_A estimates can be consistent, because in the case of the neutrino-deuteron scattering the two-body current contribution is small [8].

Theoretical models of the two-body current contribution [also called n-particles, n-holes (np-nh) in this paper] give quite different estimates of the size of the effect for both neutrino and antineutrino scattering. Recently the MB Collaboration published the first large statistics antineutrino CCQE-like (a sum of CCQE and np-nh contributions) cross section results [9]. The data have been already analyzed by the theoretical groups [10,11]. In Ref. [12] a ratio of the CCQE-like cross sections for neutrinos and antineutrinos was discussed as a function of neutrino energy. If the errors become smaller, this kind of data can allow discrimination among the models. It is important to look also for alternative ways to evaluate M_A and/or to investigate the size of the two-body current contribution. The MINERvA Collaboration analyzed the energy deposit near a CCQE-like interaction vertex looking for an evidence for multinucleon knockout events [13].

Another option is to look at the neutral current elastic (NCEL) reaction, $\nu_l + N \to \nu_l + N$, where N denotes proton or neutron. As explained in detail in Sec. II, the basic theoretical framework to investigate NCEL scattering is similar to the one used for CCQE scattering. The neutral current (NC) hadronic current is expressed in terms of the vector and axial form factors, which are linear combinations of the form factors present in the CCQE reaction with an addition of new terms sensitive to the strange quark content of nucleons. Thus, the NCEL scattering data allow for extraction of both M_A and the strange quark contribution to the form factors. In fact, most of the interest in the NCEL reaction comes from its potential to measure the strangeness of the nucleon.

The axial strange form factor can be determined from the NCEL neutrino-CH_2 scattering data because it enters proton and neutron matrix elements with opposite signs. Typically, in experiments, one tries to extract g_A^s, a value of the axial strange form factor at $Q^2 = 0$. It corresponds to the fraction of strange quarks and antiquarks that contribute to the total proton spin, commonly denoted as Δs. The first estimation based on νN data (BNL E734 experiment) was done in Ref. [14] with the result $g_A^s = -0.15 \pm 0.09$. For the later discussions see Refs. [15,16].

About three years ago the MB Collaboration measured the flux averaged NCEL differential cross section on the CH_2 target [17]. Two observables were considered. The first one is the distribution of events in the total reconstructed kinetic energy of the final state nucleons. The measurement is based on the MB detector ability to analyze the scintillation light in the absence of Cherenkov light from the final state muon. In the second observable a proton enriched sample of events is analyzed with kinetic energies above the Cherenkov radiation threshold. The observable is defined as the ratio of the cross section for the proton enriched sample to the total NCEL-like (events with no pions in the final state) cross section. The MB Collaboration made two separate parameter extractions. Assuming $g_A^s = 0$ the value of $M_A^{\mathrm{eff}} = 1.39 \pm 0.11$ GeV was obtained from the first observable. Taking the value $M_A^{\mathrm{eff}} = 1.35$ GeV from the CCQE analysis [2], MB found $g_A^s = 0.08 \pm 0.26$ from the proton enriched sample of events. The description of both data samples in terms of $M_A^{\rm eff} \sim 1.35$ GeV and $g_A^s \sim 0$ is consistent. The MB Collaboration did not attempt to make a simultaneous fit to both theoretical parameters (such fits were only discussed in Ref. [18]).

In the MB analysis the values of M_A used in modeling scattering off carbon and off free protons were different. For protons the M_A was fixed to be 1.13 GeV. For carbon the axial mass value was treated as a free parameter. A large *effective* M_A value is expected to account for the np-nh contribution present in neutrino-carbon scattering but absent in the neutrino-proton scattering. MB Collaboration used the NUANCE neutrino event generator with nuclear effects described by the Fermi gas model and final state interactions (FSIs) [19]. NUANCE does not include the np-nh contribution.

The data from Ref. [17] have been already discussed in some phenomenological papers. Butkevich and Perevalov [20] investigated an impact of a more realistic nuclear model in the MB data analysis. A relativistic distorted wave impulse approximation [21] model leads to the values $M_A = 1.28 \pm 0.05$ GeV and $g_s^A = -0.11 \pm 0.36$, consistent with those reported in Ref. [17]. The spectral function formalism was used by Ankowski in Ref. [22], with the conclusion that the shape of the MB measured distribution of events in Q^2 is reproduced with $M_A^{\rm eff} = 1.23$ GeV. However, there is a 20% discrepancy in the overall normalization with the MB results (the measured cross section is larger). Meucci, Giusti, and Pacati analyzed the predictions of four nuclear models [23]. It turned out that the relativistic Green function model is able to reproduce the MB NCEL data with the value of M_A close to those obtained in old deuteron-target experiments.

The purpose of this paper is to perform the first analysis of the MB NCEL data using a model that includes the np-nh contribution. The model is provided by the NuWro Monte Carlo event generator [24] developed over last nine years at Wrocław University. NuWro describes the neutral current np-nh contribution with the effective transverse enhancement (TE) model [7]. The TE model provides the contribution to the neutrino inclusive cross section and predictions for the final state nucleons are obtained with a procedure described in Ref. [25]. The advantage of the TE model is that it can be safely used for neutrinos of energies larger than 1.5 GeV. In this paper only nucleons resulting from the np-nh events are analyzed and differences between microscopic (see Refs. [4,5]) and effective np-nh models are made smaller by Fermi motion and final state interactions effects. The recent MINERvA CCQE-like data analysis demonstrates that with $M_A = 0.99$ GeV and the TE model both neutrino and antineutrino Q^2 distributions are well reproduced [13].

Another important difference with respect to the previous studies of the MB NCEL data is in the treatment of nuclear effects. We compare NuWro predictions to the quantities (visible energy) that are directly observable and we do not rely on the NUANCE FSI model.

Our main result is a simultaneous fit to the M_A and g_A^s done using the MB data for the distribution of events in the total reconstructed kinetic energy of the final state nucleons, with the outcome $M_A = 1.10^{+0.13}_{-0.15}$ GeV and $g_A^s = -0.4^{+0.5}_{-0.3}$. We argue that the second MB observable is very sensitive to details of FSI and the np-nh kinematics model and it is very difficult to use it as a reliable source of information about theoretical model parameters. On the contrary, the first observable is quite robust to such details and can be successfully used to extract values of the interesting quantities.

Our paper is organized as follows: in Sec. II a general description of the NCEL reaction is given; in Sec. III the main features of the NuWro generator are summarized; Sec. IV contains details of the data analysis and the MB energy unfolding procedure; in Sec. V we present our main results; and conclusions can be found in Sec. VI.

II. ELASTIC NEUTRAL CURRENT REACTION FORMALISM

We consider neutral current neutrino-nucleon scattering:

$$\nu(k) + N(p) \to l'(k') + N'(p'), \tag{1}$$

where N, N', l' denote the initial and final state nucleons and the outgoing lepton with the four-momenta, p, p', and k', respectively. The four-momentum transfer is given by $q^\mu \equiv k^\mu - k'^\mu = (\omega, \mathbf{q})$, $Q^2 \equiv -q^2$.

In the Born approximation the scattering matrix element factorizes into the product of leptonic and hadronic contributions:

$$i\mathcal{M}_{nc}^{(1)} \approx -i\frac{G_F}{\sqrt{2}} j_\mu h_{nc}^\mu, \quad Q^2 \ll M_Z^2, \tag{2}$$

where θ_C is the Cabibbo angle, G_F is the Fermi constant, and j_μ and $h_{cc,nc}^\mu$ are the expectation values of the leptonic and hadronic currents. The leptonic part is

$$j_\mu = \bar{u}(k')\gamma^\mu(1-\gamma_5)u(k), \tag{3}$$

while getting the hadronic contribution requires an extra phenomenological input in the general formula

$$h^\mu(q) = \overline{u}(p')\Gamma^\mu(q)u(p), \tag{4}$$

with the effective hadronic vertex Γ^μ.

To construct Γ^μ for the NCEL scattering, one has to follow the pattern given by the Standard Model. The CVC theory, the PCAC hypothesis, and the $SU(2)$ isospin symmetry relate the neutral current form factors to those present in the electromagnetic and charged current hadronic matrix elements [26]. The NC hadronic vertex reads

$$\Gamma^\mu_{{\rm NC},p(n)} = \gamma^\mu F_1^{{\rm NC},p(n)} + \frac{i\sigma^{\mu\nu}q_\nu}{2M}\gamma^\mu F_2^{{\rm NC},p(n)} - \gamma^\mu\gamma_5 G_A^{{\rm NC},p(n)}, \tag{5}$$

where indices p and n refer to proton and neutron. The NC form factors can be expressed as

$$F_{1,2}^{{\rm NC},p(n)}(Q^2) = \pm\tfrac{1}{2}\{F_{1,2}^p(Q^2) - F_{1,2}^n(Q^2)\} - 2\sin^2\theta_W F_{1,2}^{p(n)}(Q^2) - \tfrac{1}{2}F_{1,2}^s(Q^2), \tag{6}$$

$$G_A^{{\rm NC},p(n)}(Q^2) = \pm\tfrac{1}{2}G_A(Q^2) - \tfrac{1}{2}G_A^s(Q^2), \tag{7}$$

where $+(-)$ signs refer to proton (neutron), θ_W is the Weinberg angle, and $\sin^2\theta_W = 0.231$. $F_{1,2}^{p(n)}$ are the proton (neutron) electromagnetic form factors, G_A is the axial nucleon form factor,

$$G_A(Q^2) = \frac{g_A}{\left(1 + \frac{Q^2}{M_A^2}\right)^2}, \quad g_A = 1.267, \tag{8}$$

and $F_{1,2}^s$ and G_A^s are the vector and the axial strange form factors.

The electromagnetic form factors F_1, F_2 are obtained from the analysis of the elastic eN scattering data (for a review see Ref. [27]) and can be expressed in terms of the electric and magnetic form factors:

$$F_1^{p(n)}(Q^2) = \frac{4M^2}{Q^2 + 4M^2}\left[G_E^{p(n)}(Q^2) + \frac{Q^2}{4M^2}G_M^{p(n)}(Q^2)\right], \tag{9}$$

$$F_2^{p(n)}(Q^2) = \frac{4M^2}{Q^2 + 4M^2}\left[G_M^{p(n)}(Q^2) - G_E^{p(n)}(Q^2)\right], \tag{10}$$

where $M = \frac{1}{2}(M_p + M_n)$ is the average nucleon mass.

In the Breit frame the electric ($G_E^{p(n)}$) and the magnetic ($G_M^{p(n)}$) nucleon form factors are related to the nucleon electric charge and current distributions. For instance, for the electric proton form factor $G_E^p(Q^2) \sim G_E^p(0) + \frac{\langle r_p^2 \rangle}{6}Q^2 + O(Q^4)$, where $\langle r_p^2\rangle = -6\frac{dG_E^p}{dQ^2}|_{Q^2=0}$ is the mean-square radius of the charge distribution.

Similarly, one can introduce the electric (G_E^s) and magnetic (G_M^s) isoscalar strange form factors. In the first approximation one can assume that the "effective sizes" of the proton and neutron strange sea are the same; therefore, we use the same strange form factors for both nucleons. The latest global analysis of the elastic parity violating ep and BNL E734 neutrino scattering data indicates that the values of vector strange form factors are consistent with zero [28], and in our analysis we set $G_{E,M}^s = 0$.

To estimate the axial strange form factor we assume that the radius of the strange sea is comparable with the axial "charge" radius of the proton so that

$$G_A^s(Q^2) = \frac{g_A^s}{\left(1 + \frac{Q^2}{M_A^2}\right)^2}, \tag{11}$$

with the free parameter g_A^s that has to be extracted from the data.

In our numerical analysis we use the BBBA05 vector form factors (from Bradford, Bodek, Budd, and Arrington [29]). We also investigate a possible impact on the results from the form factors corrected by the two-photon exchange effect [30].

III. NUWRO MONTE CARLO EVENT GENERATOR

A. Generalities

NuWro is a Monte Carlo event generator developed at Wrocław University [24]. It simulates neutrino-nucleon and neutrino-nucleus interactions, including (quasi)elastic scattering, pion production through $\Delta(1232)$ resonance (with a contribution from the nonresonant background), more inelastic processes, and coherent pion production. NuWro covers a neutrino energy range from ∼100 MeV to TeV. There are three basic nucleus models implemented in NuWro: the global or local relativistic Fermi gas model, the spectral function, and the effective momentum and density dependent potential. In the analysis described in this paper we use the local Fermi gas model. In the impulse approximation picture, all the hadrons arising at a primary vertex are propagated through the nuclear matter using the NuWro cascade model. NuWro is the open-source project and the code is freely available [31].

B. Two-body current contribution

There are three charged current (CC) two-body current models implemented in NuWro: the Instituto de Física Corpuscular (IFIC) model [5], the Martini *et al.* model [4], and the TE model [7]. In all of them the double differential cross section contribution for the final state muons is the external input and the hadronic part is modeled using the following scheme (proposed in Ref. [25]):

(i) Set randomly the four-momenta (p_1 and p_2) of the initial nucleons from the Fermi sphere with a radius determined by the local nuclear density.

(ii) Calculate the four-momentum of the hadronic system

$$W = p_1 + p_2 + q,$$

where q is the four-momentum transferred to the hadronic system.

(iii) Repeat steps 1 and 2 until the invariant hadron mass is larger than the mass of two nucleons ($W^2 > (2M)^2$).

(iv) Make the Lorentz boost to the hadronic center of mass system.

(v) Select isotropically momenta of two final state nucleons.

(vi) Boost back to the laboratory frame.

(vii) Apply final state interactions.

Results from three models depend on the distribution of events in the energy transfer. The differences are smeared out by the Fermi motion and the FSI effects.

In our analysis of the NCEL data we use the TE model [7], because to date this is the only NC np-nh model available in NuWro. In the TE model the np-nh contribution to the NC scattering cross section on carbon is introduced by the modification of the vector magnetic form factors:

$$G_M^{p,n} \to \tilde{G}_M^{p,n} = \sqrt{1 + AQ^2 \exp\left(-\frac{Q^2}{B}\right)}\,G_M^{p,n}(Q^2), \tag{12}$$

where $A = 6$ GeV^{-2} and $B = 0.34$ GeV^2. Using $\tilde{G}_M^{p,n}$ in the NCEL differential cross section formula one obtains a cross section for a sum of the NCEL and np-nh reactions. The np-nh cross section is obtained by subtracting the NCEL part described with the standard magnetic form factors:

$$\frac{d^2\sigma^{\rm MEC}}{dq d\omega} \equiv \frac{1}{2}\left\{\left(\frac{d^2\sigma^{\rm NCE}}{dqd\omega}(\tilde{G}_M^p) - \frac{d^2\sigma^{\rm NCE}}{dqd\omega}(G_M^p)\right) + \left(\frac{d^2\sigma^{\rm NCE}}{dqd\omega}(\tilde{G}_M^n) - \frac{d^2\sigma^{\rm NCE}}{dqd\omega}(G_M^n)\right)\right\}. \tag{13}$$

The value of the axial mass in the TE model is set to be $M_A^{np\text{-}nh} = 1014$ MeV, as assumed in Ref. [7]. The total cross

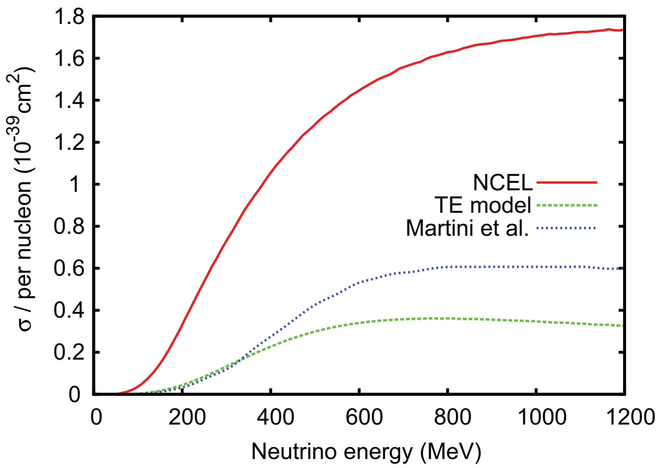

FIG. 1. (Color online) Total cross section per nucleon as a function of a neutrino energy for NC scattering off carbon: NuWro model with $M_A = 1.03$ GeV and Martini *et al.* [4].

section for the NC np-nh scattering is shown in Fig. 1. At the typical MB flux neutrino energies, $E_\nu \sim 700$ MeV, the np-nh contribution in the TE model amounts to about 19% of the NCEL cross section. For comparison we show also the predictions from the Martini *et al.* model taken from Ref. [4]. The Martini *et al.* model predicts much larger np-nh cross section. Also for the CC np-nh reaction the predictions from this model are larger than those from the IFIC and TE models.

In the CC np-nh reactions there can be either a neutron-neutron (n-n) or a proton-neutron (n-p) pair in the initial state. The probability of the mixed isospin pair is defined in NuWro by a parameter $p_{\rm CC}$, with the default value $p_{\rm CC} = 0.6$. For the NC np-nh interactions every isospin initial state pair is possible (n-p, n-n, p-p). To keep the same proportion between n-n and p-n pairs and assuming the same probability to have n-n and p-p pairs, we introduce the parameter $p_{\rm NC} = (2/p_{\rm CC} - 1)^{-1}$, giving the likelihood of a n-p pair to be selected in a NC two-body current reaction.

C. NuWro cascade model

Hadrons resulting in the primary vertex propagate through the nuclear matter with the NuWro cascade model:

(i) Nucleons are assumed to be in the potential well of depth $V = V_0 + E_F$, where E_F is the Fermi energy and $V_0 = 7$ MeV.
(ii) The formation zone (FZ) can be applied (FZ is set to be zero for the np-nh events) and the following steps are repeated:
  (a) A nucleon free path (λ) is drawn from the exponential distribution taking into account the nucleon-nucleon cross section and the local nuclear density.
  (b) If $\lambda \leqslant \lambda_{\rm max} = 0.2$ fm the nucleon is propagated by λ, the interaction kinematics is generated, and a check for Pauli blocking is done to decide if the interaction happened.
  (c) If $\lambda > \lambda_{\rm max}$ the nucleon is propagated by $\lambda_{\rm max}$.

In the cascade the Fermi motion of target nucleons is taken into account, and every new nucleon, which participates in the cascade, brings in an extra kinetic energy. When a nucleon leaves the nucleus, its kinetic energy is reduced by V setting it on-shell. If the kinetic energy is smaller than V, the nucleon is assumed to be stuck inside the nucleus.

For a more detailed description of the NuWro cascade model see Ref. [24].

IV. DATA ANALYSIS

We are going to discuss two data samples provided by the MB Collaboration. The first one (the NCEL sample) contains the distribution of the total reconstructed kinetic energy of all nucleons in the final state, normalized to the number of events seen in the detector.

The second data sample (the NCEL high energy sample) is provided in a form of the ratio

$$\eta = \frac{\tilde{X}(\nu p \to \nu p)}{X(\nu N \to \nu N)}, \quad (14)$$

where $\tilde{X}$ denotes a contribution from a special class of events, called single proton or proton enriched events. Those are the events with visible Cherenkov light and proton angle $\theta < 60^\circ$. In MC simulations the largest contribution to those events comes from the NCEL scattering on protons, which then do not undergo reinteractions. In the case of multiple proton events, the energy of an individual proton is in general too low to produce the Cherenkov light. Even if a high energy proton appears in the multiple proton event, it has typically larger scattering angle than protons unaffected by FSI. The denominator (X) denotes the contribution from all the NCEL-like interactions.

Both data samples are presented as a function of reconstructed energy[1] (ν), measured in the detector. To compare those data with the theoretical predictions given in terms of the true kinetic energy (μ), one needs the unfolding procedure, allowing a passage from μ to ν.

In the next sections we describe the original MB unfolding procedure. We had to propose a treatment of np-nh events not considered in the MB analysis.

A. MiniBooNE procedure

For all but np-nh events we follow closely the approach proposed by Perevalov in Ref. [18]. A similar unfolding procedure is used in both data samples. Five types of events giving contribution to the final distributions are considered:

(i) NCEL on hydrogen,
(ii) NCEL on a proton from carbon unaffected by FSI effects,
(iii) NCEL on a proton from carbon with FSI effects,
(iv) NCEL on a neutron from carbon, and
(v) irreducible background (pions produced in a primary vertex and absorbed due to FSI effects).

[1] We keep the original notation from Ref. [18].

The probabilities of scenarios (ii)–(v) depend on the details of the cascade models implemented in NUANCE or in NuWro.

For each type of the signal events, $k = 1, 2, \ldots, 5$, there is a response matrix ($R^{(k)}$) provided in Ref. [32], which simulates the energy smearing and the detector efficiency and defines a relation between true and reconstructed energy distributions:

$$\nu_j^{(k)} = \sum_i R_{ij}^{(k)} \mu_i^{(k)}. \quad (15)$$

$R^{(k)}$ are either 51×51 or 30×30 matrices for the two data samples, respectively. The columns of matrices label the true kinetic energy bins and rows label the reconstructed energy. There are 50 bins starting from 0 MeV up to 900 MeV plus an extra overflow bin for the NCEL sample in the true kinetic energy. For the NCEL high energy sample there are 28 bins, starting from 300 MeV up to 900 MeV plus underflow and overflow bins.

To obtain the reconstructed kinetic energy distribution and compare with the data from Ref. [17] one goes through the following steps:

(i) Use a theoretical model and calculate the flux-averaged distributions for five different types of signal events using the same bins as in the response matrices.

(ii) Use the proper response matrices to translate each histogram to the reconstructed kinetic energy distribution.

(iii) Sum all the histograms and add the background events ($\nu^{\rm BKG}$ contains dirt, beam-unrelated, and other backgrounds provided by the MB Collaboration in Ref. [32]) to get the total reconstructed energy spectrum:

$$\nu_j^{\rm MC} = \sum_i R_{ij}^{(1)} \mu_i^{(1)} + \sum_i R_{ij}^{(2)} \mu_i^{(2)} + \sum_i R_{ij}^{(3)} \mu_i^{(3)} + \sum_i R_{ij}^{(4)} \mu_i^{(4)} + \sum_i R_{ij}^{(5)} \mu_i^{(5)} + \nu_j^{\rm BKG}. \quad (16)$$

(iv) Use the provided error matrices (M_{ij}) to calculate χ^2:

$$\chi^2 = \sum_i \sum_j \left(\nu_i^{\rm DATA} - \nu_i^{\rm MC}\right) M_{ij}^{-1} \left(\nu_j^{\rm DATA} - \nu_j^{\rm MC}\right). \quad (17)$$

Unlike in the CCQE MB data published in Ref. [2], the flux normalization error is already included in the error matrix M_{ij}.

B. Our procedure

An alternative way to convert the true kinetic energy to the reconstructed one is to translate it on an event-by-event basis. For each value of the true kinetic energy the corresponding column in the response matrix gives a probability distribution with the information how the given true energy value is smeared out in the detector, normalized to the efficiency. To obtain the reconstructed kinetic energy distribution one proceeds as follows:

(i) For each event calculate the total true kinetic energy of all nucleons in the final state (μ) and get a bin number j.

(ii) Find the type of signal (k); see Sec. IV A.

(iii) Choose the jth column of the $R^{(k)}$ response matrix as the probability distribution.

(iv) Use the MC method to decide if the event is accepted (according to the efficiency) and what energy is visible in the detector.

1. *The unfolding procedure for two-body current events*

In the np-nh events there are typically two nucleons after a primary interaction and both of them propagate independently through the nucleus. In the MB analysis there are no np-nh events included and no response matrices were prepared for them. To take two-body current events into account, we must express them in terms of the five signals defined by the MB.

A naive interpretation may suggest a treatment of each nucleon from the np-nh events separately. However, it would be incorrect. The signal is recorded by photomultiplier tubes (PMTs), which absorb the light emitted in the scintillator (and also the Cherenkov radiation). The event is accepted if there is a sufficient number of PMT hits. Any of two individual nucleons may have too low energy to generate enough PMT hits, but together they can make it [33].

In our analysis we treated both nucleons from a two-body current event together and summed up the kinetic energies of all the nucleons in the final state as if they were coming from only one nucleon. In the detector np-nh events are seen as multiple proton events, so as signals (c), NCEL on proton from carbon affected by FSI effects, and (d), NCEL on neutron from carbon.

One expects events without a proton in the final state to be more smeared out in the detector, and we apply a response matrix for the signal (d) if there are two neutrons in the primary vertex or for the signal (c) in other cases [33].

In np-nh events the energy transferred to the hadronic system is shared by two nucleons, and the probability that there will be a proton with energy large enough to produce the Cherenkov light is low. Thus, the np-nh events make the ratio η [Eq. (14)] smaller.

V. RESULTS

A. Analysis without np-nh contribution

We first repeat the analysis without the np-nh contribution to check if our numerical procedures reproduce the MB results.

We assumed a fixed value of the axial mass for hydrogen, $M_A = 1.03$ GeV, and we minimized the χ^2 function for the effective axial mass for carbon ($M_A^{\rm eff}$) using the data for the reconstructed energy distribution. Following the MB procedure we fixed the value $g_A^s = 0$. The value $M_A^{\rm eff} = 1.47 \pm 0.10$ GeV was obtained with $\chi^2_{\rm min}/$ DOF $= 23.6/50$ [a confidence level (CL) of 99.9%]. This value is larger than the one reported by the MB Collaboration ($M_A^{\rm eff} = 1.39 \pm 0.11$ GeV) [17] but consistent within the 1σ error bars. A discrepancy is probably caused by the presence of the pionless $\Delta(1232)$ resonance decays in the NUANCE but not in the NuWro generator. Moreover, we use a lower value of M_A for hydrogen than the MB Collaboration.

To investigate a possible impact of the choice of the electromagnetic form factors parametrization on the final results, we repeated the computations using the form factors corrected by a two-photon exchange [30] and obtained almost identical results.

Using the data for the ratio η [Eq. (14)] we examined the strange quark contribution to the NCEL cross section. We assumed a fixed value of the axial mass: 1.03 GeV for hydrogen and an effective value of 1.47 GeV for carbon. We found the strange quark contribution to be $g_A^s = 0.24 \pm 0.46$ with $\chi^2_{\rm min}/$ DOF $= 26.7/29$ (CL 58.8%). This result is consistent with values published by the MB Collaboration [17] and the BNL E734 experiment [14].

B. Analysis with *n*p-*n*h contribution

Following the same steps the analysis was repeated including the np-nh contribution. Assuming $g_A^s = 0$ the minimum of the χ^2 for the distributions of the total reconstructed kinetic energy of the final state nucleons was found for the axial mass value $M_A = 1.15 \pm 0.11$ GeV with $\chi^2_{\rm min}/$ DOF $=$ 24.4/50 (CL 99.9%). The extraction of the strangeness from the ratio η, assuming $M_A = 1.15$ GeV, leads to the value $g_A^s = -0.72 \pm 0.55$ with $\chi^2_{\rm min}$/DOF $= 28.7/29$ (CL 48.1%), which is inconsistent with zero (as assumed in the first fit). As it was discussed before, the two-body current events contribute mostly to the denominator of the ratio η, making its value smaller. Also, a lower M_A makes the ratio η smaller. To compensate for both effects a lower value of g_A^s can be expected.

1. *Simultaneous extraction of M_A and g_A^s*

The inconsistency described in the previous subsection encouraged us to try to make a simultaneous fit of both theoretical model parameters. In the case of the first observable we obtained the following results:

(i) without np-nh events,

$$M_A = 1.34^{+0.18}_{-0.10}\ \text{GeV} \quad \text{and} \quad g_A^s = -0.5^{+0.2}_{-0.2}$$

with $\chi^2_{\rm min}/$ DOF $= 22.0/50$;

(ii) with np-nh events,

$$M_A = 1.10^{+0.13}_{-0.15}\ \text{GeV} \quad \text{and} \quad g_A^s = -0.4^{+0.5}_{-0.3}$$

with $\chi^2_{\rm min}/$ DOF $= 22.7/50$.

In the case of the second observable we discovered that the best fit values are very sensitive to many details of the theoretical model:

(i) From Fig. 4 it is clearly seen that the ratio η depends strongly on "other backgrounds."

(ii) Above 350 MeV of the kinetic energy a significant contribution comes from irreducible background (pion production and absorption) known with a precision not better than 20–30%.

(iii) We constructed Monte Carlo np-nh toy models based on the TE model with modified distribution of energy transfer, and the obtained best fit values depend strongly on such modifications; however, the results from the first observable are affected in a much weaker way.

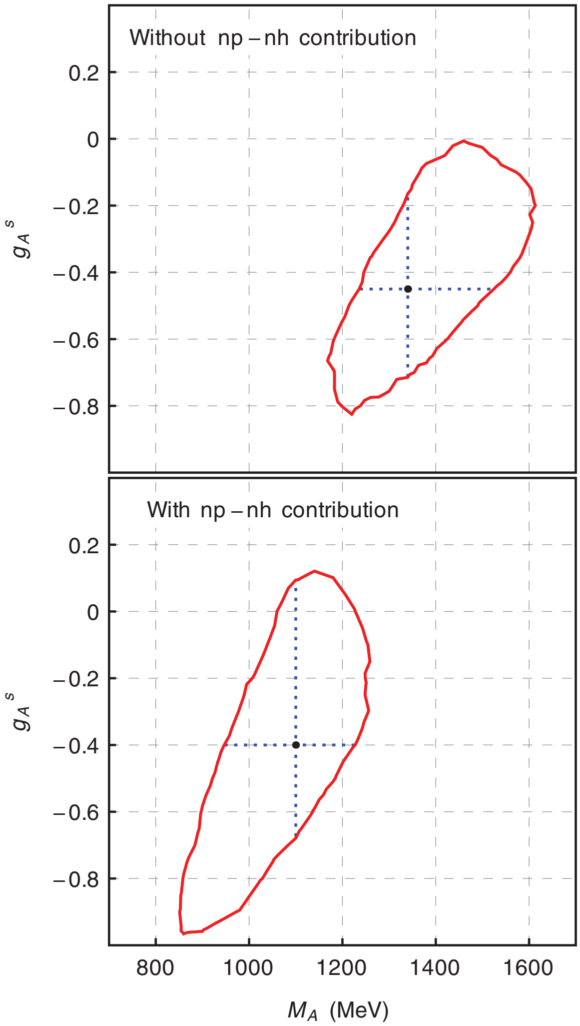

FIG. 2. (Color online) 1σ error contour for (M_A, g_A^s) parameters obtained from χ^2 [Eq. (17)], but only for the total reconstructed kinetic energy of the final state nucleons. Dots denote χ^2 minima.

Figure 2 shows our results for the simultaneous two-dimensional fits without and with the np-nh contribution included in the NuWro simulations together with 68% confidence regions. The inclusion of the np-nh events makes the best fit result for M_A consistent with the world average. It confirms that the difference between recent and older axial mass measurements can be explained by taking into account two-body current contribution. The value of the strange quark contribution is found to be consistent with zero.

We calculated the value of χ^2 for the second MB observable with the values $M_A = 1.10$ and $g_A^s = -0.4$ and obtained χ^2/DOF $= 30.2/29$. It means that the reported values are consistent also with the proton enriched sample observable.

Our best fit for the distribution of the total reconstructed kinetic energy of the final state nucleons and the overall NuWro prediction (broken down to individual contributions

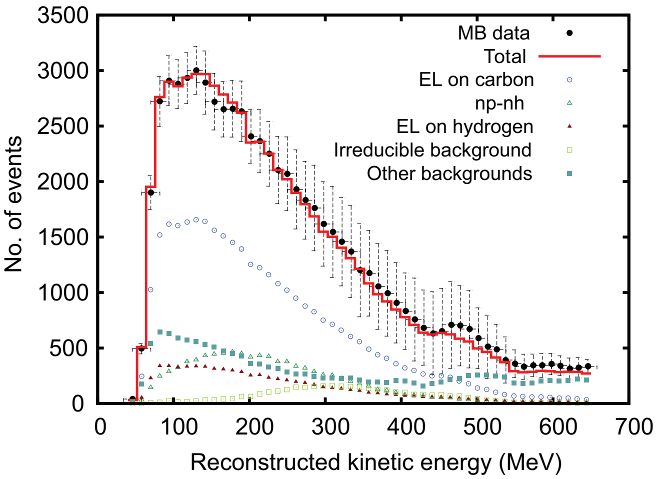

FIG. 3. (Color online) The distribution of the total reconstructed kinetic energy of the final state nucleons, broken down to individual contributions from elastic scattering on carbon, np-nh, elastic scattering on hydrogen, irreducible background, and other backgrounds. The NuWro result is obtained with the $M_A = 1.10$ GeV and $g_A^s = -0.4$ values.

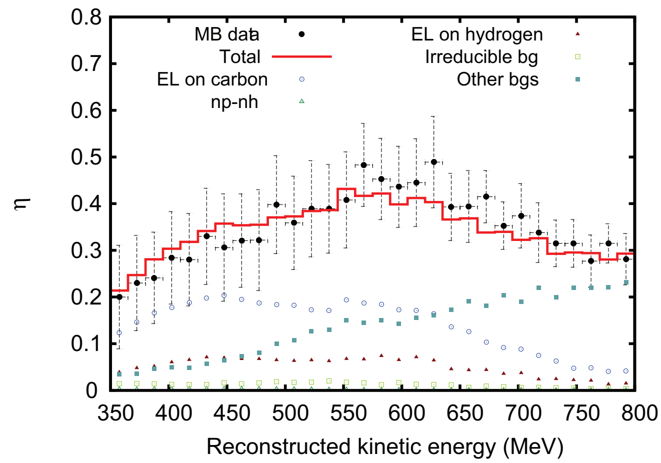

FIG. 4. (Color online) The ratio η [Eq. (14)] as a function of the total reconstructed kinetic energy of all nucleons in the final state, broken down to individual contributions from elastic scattering on carbon, np-nh, elastic scattering on hydrogen, irreducible background, and other backgrounds. The NuWro result is obtained with the $M_A = 1.10$ GeV and $g_A^s = -0.4$ values.

from elastic scattering on carbon, elastic scattering on hydrogen, two-body current, irreducible background, and other backgrounds) is demonstrated in Fig. 3. The contribution coming from the two-body current amounts to approximately 15% of the overall distribution, affecting both its shape and the normalization. As we focus on the sum of the kinetic energies of all the nucleons in the final state, the result is not very sensitive to the assumptions made on the np-nh kinematics described in Sec. III B.

Our predictions for the ratio η obtained with the values $M_A = 1.10$ and $g_A^s = -0.4$ together with the contributions to the numerator coming from various signal events are presented in Fig. 4.

As mentioned in Sec. III C the formation zone for the np-nh events is assumed to be zero, because there is no clear physical motivation to introduce it. To estimate how important the FZ effect can be for the NCEL analysis we repeated the computations assuming the FZ for the np-nh events to be 1 fm. It turned out that this assumption does not affect the final results in a statistically relevant way.

We investigated the impact of the uncertainty of the value of the parameter p_{CC} defining a relative abundance of n-p and n-n pairs on which two-body current scattering occurs. The default value of p_{CC} is 0.6 and we repeated the computations with the value $p_{CC} = 0.9$. No influence on the final results was found.

VI. CONCLUSIONS AND OUTLOOK

The impact of the two-body current events on the analysis of the MB data for the neutrino NCEL scattering on CH_2 was investigated in detail. This is the first analysis of this kind yet. We performed a simultaneous fit to two theoretical model parameters and obtained the values $M_A = 1.10^{+0.13}_{-0.15}$ GeV and $g_A^s = -0.4^{+0.5}_{-0.3}$. Our results provide new evidence that large axial mass measurements can be explained by the two-body current contribution to the cross section neglected in the experimental data analysis.

It would be interesting to repeat this analysis using one of the microscopic models of the NC two-body current contribution. Also, it is desirable to include other nuclear effects like random phase approximation (RPA) correlations. As mentioned above, NuWro contains implementations of IFIC and Martini *et al.* models for np-nh in the CC channel only. Recently, using the theoretical computations from [34] NuWro was upgraded with the implementation of RPA, but again only for the CC reactions. We are planning to include np-nh dynamics and the RPA effects for NC channels but it requires a significant amount of theoretical and programming work. For the RPA an appropriate recalculation of the components of the polarization tensor is needed as in the relativistic formalism adopted in Ref. [34] where the response functions are calculated in the analytical form.

Recently the MiniBooNE Collaboration made public the preliminary results from the antineutrino NCEL analysis [12]. They are supplementary to those discussed in this paper. When the data become available a combined analysis will have more potential to investigate the np-nh contribution and put more constraints on the g_A^s value.

As discussed in Sec. V B the MB proton enriched distribution of events contains important information about hadrons resulting from np-nh events not explored in this study. To make use of this information a very good control over the FSI effects is required.

Finally, we would like to note that there is an interesting idea for an alternative measurement of the NCEL cross section described in Ref. [35]. The authors investigate the relation between the rate of the observed γ rays coming from nuclear deexcitation in water-Cherenkov detectors and the NCEL cross section.

ACKNOWLEDGMENTS

We would like to thank Denis Perevalov, Arie Bodek, and Eric Christy for useful information. The authors were partially supported by Grant No. UMO-2-11/M/ST2/02578. Most of the numerical calculations were carried out in the Wrocław Centre for Networking and Supercomputing (http://www.wcss.wroc.pl), Grant No. 268.

[1] K. Abe *et al*. (T2K Collaboration), Nucl. Instrum. Meth. A **659**, 106 (2011).
[2] A. A. Aguilar-Arevalo *et al*. (MiniBooNE Collaboration), Phys. Rev. D **81**, 092005 (2010).
[3] V. Bernard, L. Elouadrhiri, and U. G. Meissner, J. Phys. G **28**, R1 (2002).
[4] M. Martini, M. Ericson, G. Chanfray, and J. Marteau, Phys. Rev. C **80**, 065501 (2009).
[5] J. Nieves, I. R. Simo, and M. J. Vicente Vacas, Phys. Rev. C **83**, 045501 (2011).
[6] M. Martini, M. Ericson, G. Chanfray, and J. Marteau, Phys. Rev. C **81**, 045502 (2010); J. Nieves, I. Ruiz Simo, and M. J. Vicente Vacas, Phys. Lett. B **707**, 72 (2012); A. Meucci and C. Giusti, Phys. Rev. D **85**, 093002 (2012); J. E. Amaro, M. B. Barbaro, J. A. Caballero, T. W. Donnelly, and J. M. Udias, *ibid*. **84**, 033004 (2011).
[7] A. Bodek, H. S. Budd, and M. E. Christy, Eur. Phys. J. C **71**, 1726 (2011).
[8] G. Shen, L. E. Marcucci, J. Carlson, S. Gandolfi, and R. Schiavilla, Phys. Rev. C **86**, 035503 (2012).
[9] A. A. Aguilar-Arevalo *et al*. (MiniBooNE Collaboration), Phys. Rev. D **88**, 032001 (2013).
[10] M. Martini and M. Ericson, Phys. Rev. C **87**, 065501 (2013).
[11] J. Nieves, I. R. Simo, and M. J. V. Vacas, arXiv:1302.0703.
[12] J. Grange and R. Dharmapalan, a talk at NuInt12, Rio de Janeiro, 2012 (unpublished).
[13] G. A. Fiorentini *et al*. (MINERvA Collaboration), Phys. Rev. Lett. **111**, 022502 (2013); L. Fields *et al*. (MINERvA Collaboration), *ibid*. **111**, 022501 (2013).
[14] L. A. Ahrens *et al*., Phys. Rev. D **35**, 785 (1987).
[15] G. T. Garvey, W. C. Louis, and D. H. White, Phys. Rev. C **48**, 761 (1993).
[16] W. M. Alberico, M. B. Barbaro, S. M. Bilenky, J. A. Caballero, C. Giunti, C. Maieron, E. Moya de Guerra, and J. M. Udias, Nucl. Phys. A **623**, 471 (1997); Phys. Lett. B **438**, 9 (1998).
[17] A. A. Aguilar-Arevalo *et al*. (MiniBooNE Collaboration), Phys. Rev. D **82**, 092005 (2010).
[18] D. Perevalov, Ph.D. thesis, University of Alabama, 2009.
[19] D. Casper, Nucl. Phys. B, Proc. Suppl. **112**, 161 (2002).
[20] A. V. Butkevich and D. Perevalov, Phys. Rev. C **84**, 015501 (2011).
[21] A. V. Butkevich and S. A. Kulagin, Phys. Rev. C **76**, 045502 (2007).
[22] A. M. Ankowski, Phys. Rev. C **86**, 024616 (2012).
[23] A. Meucci, C. Giusti, and F. D. Pacati, Phys. Rev. D **84**, 113003 (2011).
[24] T. Golan, C. Juszczak, and J. T. Sobczyk, Phys. Rev. C **86**, 015505 (2012).
[25] J. T. Sobczyk, Phys. Rev. C **86**, 015504 (2012).
[26] W. M. Alberico, S. M. Bilenky, and C. Maieron, Phys. Rep. **358**, 227 (2002).
[27] C. F. Perdrisat, V. Punjabi, and M. Vanderhaeghen, Prog. Part. Nucl. Phys. **59**, 694 (2007).
[28] S. F. Pate and J. P. Schaub, J. Phys. Conf. Ser. **295**, 012037 (2011).
[29] R. Bradford, A. Bodek, H. Budd, and J. Arrington, Nucl. Phys. B, Proc. Suppl. **159**, 127 (2006).
[30] K. M. Graczyk, Phys. Rev. C **84**, 034314 (2011); K. M. Graczyk, P. Plonski, and R. Sulej, J. High Energy Phys. 09 (2010) 053.
[31] http://borg.ift.uni.wroc.pl/nuwro/.
[32] MiniBooNE Neutral Current Elastic Data Release, http://www-boone.fnal.gov/for_physicists/data_release/ncel.
[33] D. Perevalov (private communication).
[34] K. M. Graczyk and J. T. Sobczyk, Eur. Phys. J. C **31**, 177 (2003); K. M. Graczyk, Nucl. Phys. A **748**, 313 (2005); arXiv:nucl-th/0401053.
[35] A. M. Ankowski, O. Benhar, Takaaki Mori, Ryuta Yamaguchi, and Makoto Sakuda, Phys. Rev. Lett. **108**, 052505 (2012).